THE PLANT CELL

Research Article

Natural allelic variation in a modulator of auxin homeostasis improves grain yield and nitrogen use efficiency in rice

Siyu Zhang [iD] ,[1,†] Limei Zhu [iD] ,[1,†] Chengbo Shen [iD] ,[1,†] Zhe Ji [iD] ,[2,†] Haipeng Zhang [iD] ,[1] Tao Zhang [iD] ,[3] Yu Li [iD] ,[4,5] Jianping Yu [iD] ,[4] Ning Yang [iD] ,[6] Yubing He [iD] ,[1] Yanan Tian [iD] ,[1] Kun Wu [iD] ,[4] Juyou Wu [iD] ,[1] Nicholas P. Harberd [iD] ,[2] Yunde Zhao [iD] ,[3] Xiangdong Fu [iD] ,[4,5] Shaokui Wang [iD] [7,**,‡] and Shan Li [iD] [1,8,*,‡]

1 State Key Laboratory of Crop Genetics and Germplasm Enhancement, Nanjing Agricultural University, Nanjing 210095, China
2 Department of Plant Sciences, University of Oxford, Oxford OX1 3RB, UK
3 Section of Cell and Developmental Biology, University of California, San Diego, La Jolla, California 92093, USA
4 State Key Laboratory of Plant Cell and Chromosome Engineering, Institute of Genetics and Developmental Biology, Innovation Academy for Seed Design, Chinese Academy of Sciences, Beijing 100101, China
5 College of Life Sciences, University of Chinese Academy of Sciences, Beijing 100049, China
6 National Key Laboratory of Crop Genetic Improvement and National Center of Plant Gene Research (Wuhan), Huazhong Agricultural University, Wuhan 430070, China
7 State Key Laboratory for Conservation and Utilization of Subtropical Agro-Bioresources, South China Agricultural University, Guangzhou 510640, China
8 Jiangsu Collaborative Innovation Center for Modern Crop Production, Nanjing Agricultural University, Nanjing 210095, China

*Author for correspondence: shanli@njau.edu.cn, shaokuiwang@scau.edu.cn
†These authors contributed equally to this article (S.Z., L.Z., C.S., Z.J.).
‡Senior authors.

S.Z., L.Z., C.S., Z. J., and S.L. designed the research. S.Z., L.Z., and C.S. performed most of the experiments. S.Z., L.Z., C.S., and Z.J. conducted QTL analysis and map-based cloning. S.Z., L.Z., C.S., H.Z., Y.T., and K.W. performed field experiments. Y.L. conducted ChIP-qPCR analysis and phylogenetic analysis. S.Z. performed nuclear and cellular protein separation. T.Z., N.Y., and Y.H. constructed transgenic rice plants. J.Y. performed haplotype analysis. S.W. provided SSSL lines. Z.J. and S.L. wrote the manuscript. J.W., N.P.H., Y.Z., and X.F. revised the manuscript. All authors discussed the results and contributed to the manuscript.

The authors responsible for distribution of materials integral to the findings presented in this article in accordance with the policy described in the Instructions for Authors (https://academic.oup.com/plcell/pages/General-Instructions) are Shan Li (shanli@njau.edu.cn) and Shaokui Wang (shaokuiwang@scau.edu.cn).

Abstract

The external application of nitrogen (N) fertilizers is an important practice for increasing crop production. However, the excessive use of fertilizers significantly increases production costs and causes environmental problems, making the improvement of crop N-use efficiency (NUE) crucial for sustainable agriculture in the future. Here we show that the rice (*Oryza sativa*) NUE quantitative trait locus DULL NITROGEN RESPONSE1 (*qDNR1*), which is involved in auxin homeostasis, reflects the differences in nitrate (NO_3^-) uptake, N assimilation, and yield enhancement between *indica* and *japonica* rice varieties. Rice plants carrying the *DNR1*^*indica* allele exhibit reduced N-responsive transcription and protein abundance of DNR1. This, in turn, promotes auxin biosynthesis, thereby inducing AUXIN RESPONSE FACTOR-mediated activation of NO_3^- transporter and N-metabolism genes, resulting in improved NUE and grain yield. We also show that a loss-of-function mutation at the *DNR1* locus is associated with increased N uptake and assimilation, resulting in improved rice yield under moderate levels of N fertilizer input. Therefore, modulating the *DNR1*-mediated auxin response represents a promising strategy for achieving environmentally sustainable improvements in rice yield.

IN A NUTSHELL

Background: Nitrogen (N), an essential element for crop growth, is provided to plants by external fertilizer application. However, the excessive use of N fertilizers increases the cost of agricultural production and causes a series of environmental problems including climate change, soil acidification, and water eutrophication. Therefore, improving crop N use efficiency (NUE) is an urgent goal of modern agriculture. Plant N metabolism is known to be regulated by multiple plant hormones including auxin. Nevertheless, the identities of the auxin-related genes involved in this regulation and how they can be exploited to enhance crop NUE and yield remain largely elusive.

Question: We wanted to know how *qDNR1* (*Dull Nitrogen Response 1*), a NUE-related quantitative trait locus (QTL) identified in rice, modulates N metabolism by regulating auxin homeostasis and whether manipulating DNR1 levels in this crop could improve NUE and crop yields.

Findings: *qDNR1* is a QTL responsible for the differences in N uptake and assimilation activities between *indica* and *japonica* rice varieties. *DNR1* is a negative regulator of auxin accumulation that is itself regulated by external N conditions. *Indica* rice varieties generally contain lower DNR1 levels than *japonica* rice, providing them with higher auxin contents. This, in turn, leads to increased NUE and grain yield by activating multiple AUXIN RESPONSE FACTORs. Finally, we suggest that increasing the auxin contents in *japonica* varieties by reducing their DNR1 levels could improve their NUE and grain yield.

Next steps: Our findings suggest that modulating the N-*DNR1*-mediated auxin response could be used to improve rice yield in an environmentally sustainable manner. How this breeding strategy could be implemented will be the focus of future studies. In addition, the mechanism underlying how N increases DNR1 levels would be worth exploring in the future.

Introduction

Nitrogen (N) is one of the most important nutrients for plant growth and grain yield. Accordingly, the application of N fertilizers has led to a dramatic boost in global crop yields over the last half-century (Godfray et al., 2010; Liu et al., 2013; Chen et al., 2014; Li et al., 2017). Excess N input, however, causes significant environmental damage and reduces biodiversity (Guo et al., 2010; Kaiser, 2018). Therefore, developing new crop varieties that combine high yields with improved N-use efficiency (NUE) is an urgent goal for achieving more sustainable agriculture with a minimum demand for N (Luo et al., 2020). Although ammonium (NH_4^+) is considered to be a favorable source of N for plants growing under anaerobic conditions, a significant amount of nitrate (NO_3^-; accounting for as much as 40% of total available N) is absorbed and utilized by paddy field-grown rice (*Oryza sativa*) due to the occurrence of nitrification in the rhizosphere (Li et al., 2008; Xu et al., 2012; Chen and Ma, 2015; Yang et al., 2015; Gao et al., 2019).

To date, major components involved in NO_3^- acquisition, transport, assimilation, and signal transduction in rice have been well-characterized. NO_3^- uptake is mainly mediated by the dual-affinity NO_3^- transporter OsNRT1.1B (Chen and Ma, 2015; Duan and Zhang, 2015; Hu et al., 2015a; Fan et al., 2016), the low-affinity transporter OsNPF2.4 (Xia et al., 2015), and the high-affinity transporters OsNRT2.1, OsNRT2.2, and OsNRT2.3a, which require interactions with the partner protein OsNAR2.1 (Yan et al., 2011). OsNRT1.1B and OsNPF2.4 also function in long-distance NO_3^- transport, whereas NO_3^- redistribution is mediated by OsNPF6.1 (Tang et al., 2019). Following uptake, NO_3^- is reduced to nitrite (NO_2^-) by the *OsNR2*-encoded NADH/NADPH-dependent NO_3^- reductase (NR) for NO_3^- assimilation (Gao et al., 2019).

Accumulating evidence indicates that crosstalk between plant N metabolism and several phytohormone signaling pathways, including gibberellin, auxin, cytokinin, abscisic acid, and strigolactone, affects plant growth and development (Sakakibara et al., 2006; Kiba et al., 2011; Luo et al., 2018). Therefore, adjusting the concentrations of particular phytohormones and/or modifying their signaling mediators have emerged as potential strategies for enhancing plant NUE. For example, two gibberellin-regulated transcription factors in rice, GROWTH-REGULATING FACTOR 4 (GRF4) and NITROGEN-MEDIATED TILLER GROWTH RESPONSE5 (NGR5), globally activate plant N metabolic processes and enhance N-mediated tillering, respectively, serving as targets for improving crop NUE and yield (Li et al., 2018; Wu et al., 2020). Similarly, the crosstalk between auxin and N metabolism has been investigated since the 1930s. Early studies suggested that N deficiency reduces auxin content in the above-ground tissues of plants (Avery et al., 1937; Avery and Pottorf, 1945), whereas more recently, the opposite pattern was observed in roots. Specifically, low NO_3^- levels lead to auxin accumulation in roots in *Arabidopsis thaliana*, soybean (*Glycine max*), wheat (*Triticum aestivum*), and maize (*Zea mays*), suggesting that auxin plays an important role in relaying external N availability to root growth responses (Caba et al., 2000; Walch-Liu et al., 2006; Tian et al., 2008; Ma et al., 2014). Indeed, high N levels reduce root auxin contents by modifying the transcript levels of genes involved in auxin influx (e.g. *AUX1*, *LAX2*, and *LAX3*) and efflux (e.g. *PIN1*, *PIN2*, *PIN4*, and *PIN7*). In contrast, exogenous treatment with the auxins 1-naphthaleneacetic acid (NAA) and indole-3-acetic acid (IAA) restored primary root growth in maize, even under high NO_3^- conditions that are inhibitory to root elongation (Tian et al., 2008).

In Arabidopsis, the dual-affinity NO_3^- transceptor (transporter/receptor) NRT1.1 can also transport auxin and is

essential for initiating lateral root proliferation in soil patches with high NO_3^- levels (Krouk et al., 2010). On the other hand, lateral root emergence and growth triggered by low N availability is dependent on the functional auxin biosynthetic enzyme TRYPTOPHAN (Trp) AMINOTRANSFERASE-RELATED 2 (Ma et al., 2014). Auxin signaling components have also been identified as N-responsive regulators of root architecture. NO_3^- downregulates the expression of the microRNA *miR167* while upregulating the expression of *miR393*, which targets the Auxin Response Factor (ARF) gene *ARF8* and the auxin receptor gene *AFB3*, respectively, in Arabidopsis. Consequently, mutants lacking either *ARF8* or *AFB3* exhibit a compromised root developmental response to external N (Wu et al., 2006; Gifford et al., 2008; Vidal et al., 2010). Nevertheless, although the genes involved in auxin biosynthetic and signaling pathways have been extensively studied, our knowledge of how auxin-related genes respond to the fluctuations in N availability is still very limited. Moreover, whether auxin, in turn, regulates plant N metabolism and could therefore be utilized to improve crop NUE remains to be determined.

Here, we carried out quantitative trait locus (QTL) analysis of NO_3^- uptake with a set of 71 single-segment substitution lines (SSSLs) obtained by crossing rice varieties Hua–Jing–Xian (HJX74) and IRAP9. This analysis revealed *DULL NITROGEN RESPONSE1* (*DNR1*), a candidate gene that might be involved in modulating auxin homeostasis. *DNR1* diverges between *indica* and *japonica* rice varieties, which might contribute to the difference in NO_3^- uptake activity between the two subspecies. The *indica* DNR1 variant ($DNR1^{indica}$) confers reduced DNR1 protein abundance, increased auxin accumulation, and enhanced NO_3^- uptake and assimilation. Further analysis revealed that the auxin-responsive OsARFs promote NUE and grain yield by trans-activating the expression of genes related to NO_3^- metabolism . Therefore, the DNR1–auxin–OsARFs module represents an excellent target for simultaneously improving NUE and yield potential in rice.

Results

Identification of *qDNR1* as a major QTL associated with NO_3^- uptake in rice

We previously examined the $^{15}NH_4^+$ uptake rates of 36 *semidwarf1* (*sd1*)-containing *indica* rice varieties and identified *GRF4* as a regulator of NUE (Li et al., 2018). In this study, we expanded our survey to include both *indica* and *japonica* *sd1*-containing varieties and found significant variations in their $^{15}NO_3^-$ uptake rates. For example, *indica* rice variety HJX74 exhibited much higher NO_3^- uptake activity than *japonica* variety IRAP9 (Figure 1A). Therefore, we constructed a set of 71 SSSLs by crossing IRAP9 (the donor parent) with HJX74 (the recurrent parent). Each SSSL contained a single chromosome segment from IRAP9 substituted into the HJX74 genetic background (Xi et al., 2006). Subsequent QTL analysis of these 71 SSSLs revealed two loci responsible for the reduced NO_3^- uptake rate in IRAP9. One of these

loci, *qDNR1*, was identified on the short arm of chromosome 1 defined by the markers R15 and STS-1-20.2 (Figure 1, B and D; Supplemental Data Set 1). The other locus, *qDNR10*, is located on chromosome 10 and coincides (in map position) with *OsNRT1.1B*. The variation in *OsNRT1.1B* in *indica* and *japonica* rice subspecies has been reported to contribute to the difference in their NO_3^- uptake capacities (Hu et al., 2015a).

We used 144 BC_1F_2 and 947 BC_2F_2 plants developed from a backcross between 27-055 (donor parent) and HJX74 (recurrent parent) for fine-scale mapping of *qDNR1*. The candidate region was narrowed down to ∼11-kb segment flanked by the markers DN11 and DN12, which harbors the gene promoter region of the LOC_Os01g08270 locus (Supplemental Figure S1A). Sequence comparison of the candidate gene *DNR1* revealed multiple single nucleotide polymorphisms (SNPs) and small indels (insertions/deletions) of a few base pairs (bp) between HJX74 and IRAP9, as well as a 520-bp deletion (−1,728 to −1,209 in the promoter region) in HJX74 (Supplemental Figure S1, A and B). This 520-bp segment was present in all *japonica* varieties but was absent in all *indica* varieties from our collection, which coincides with the generally lower *DNR1* transcript levels and higher NO_3^- uptake rates in *indica* compared to *japonica* (Supplemental Figure S2). Therefore, the downregulation of *DNR1*, likely conferred by the truncated *indica* DNR1 promoter, appears to promote NO_3^- uptake in rice.

Phylogenetic analysis suggested that *DNR1* is closely related to Arabidopsis *VAS1*, which encodes an aminotransferase that catalyzes the conversion of indole-3-pyruvate to L-Trp, thus antagonizing auxin biosynthesis (Supplemental Figure S3A; Zheng et al., 2013; Pieck et al., 2015). The homologous relationship between these two genes was also confirmed by a similar phylogenetic analysis reported recently (Matsuo et al., 2020). Moreover, amino acid sequence alignment indicated that DNR1 and VAS1 share high sequence similarity (Supplemental Figure S3B). Interestingly, although a previous study showed that Arabidopsis VAS1-green fluorescent protein (GFP) fusion protein localizes to the cytoplasm (Zheng et al., 2013), our analysis of both rice protoplasts transfected with DNR1 fused with GFP (DNR1–GFP) and transgenic rice plant carrying the *p35S:DNR1-GFP* construct showed that DNR1 is present in both the nucleus and cytoplasm in rice (Supplemental Figure S4, A and B). Isolation of nuclear and cellular protein extracts confirmed the presence of the DNR1–GFP fusion protein in both compartments, with the nucleus-localized transcription factor GRF4 serving as a control (Supplemental Figure S4C; Che et al., 2015; Duan et al., 2015; Hu et al., 2015b).

To investigate how the two *DNR1* variant alleles confer the variation in NO_3^- uptake observed in the two rice subspecies, we developed a near-isogenic line (NIL) in the HJX74 background that carries the *japonica* DNR1 allele from IRAP9 (NIL-$DNR1^{IRAP9}$; Figure 1E). NIL-$DNR1^{IRAP9}$ exhibited semi-dwarfism, increased tillering and reduced panicle branching, grain number, and grain yield due to the
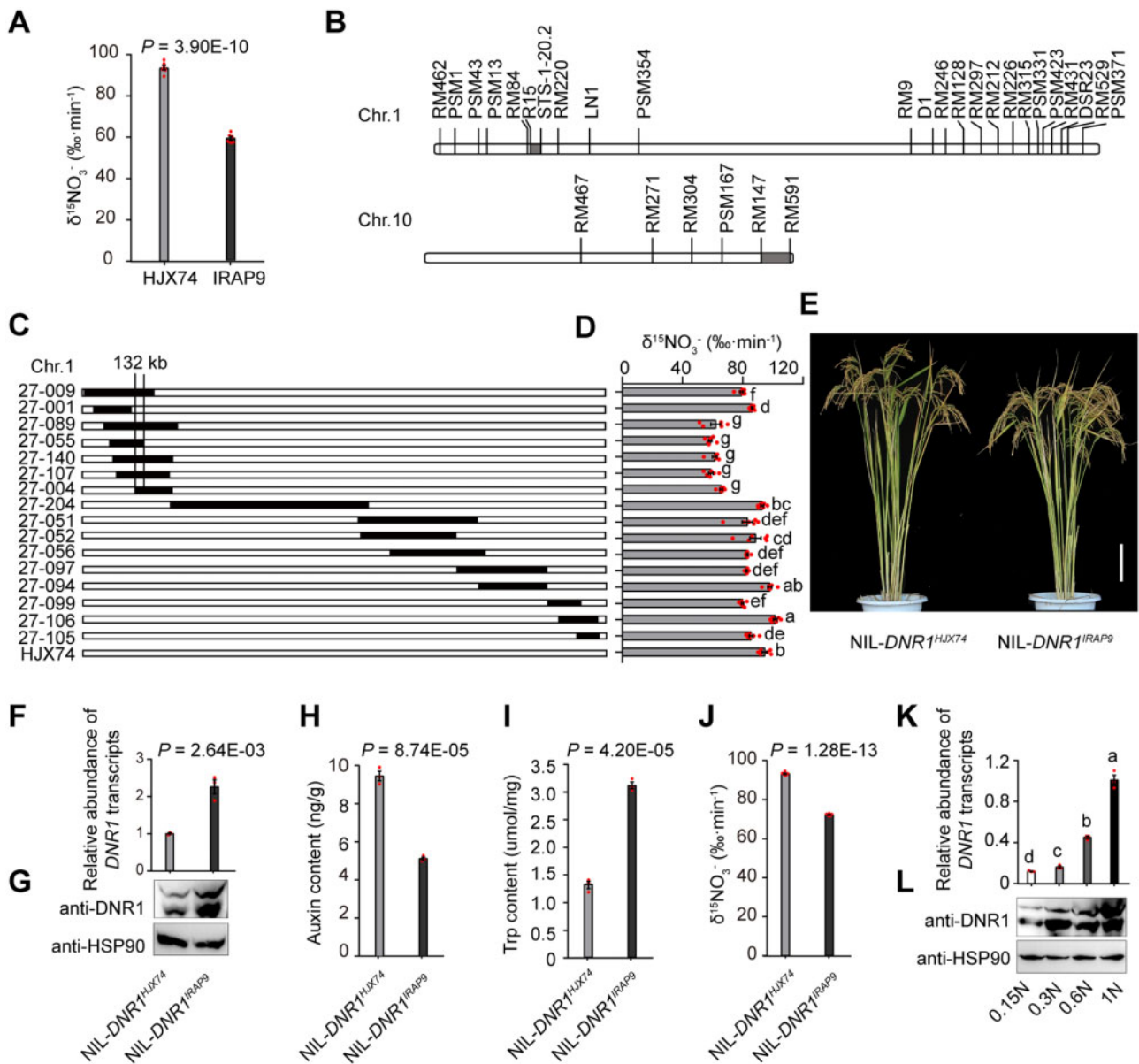
Figure 1 *DNR1*, a major QTL for NO_3^- uptake in rice, represses auxin accumulation and is N-responsive. (A) $^{15}NO_3^-$ uptake rates of the parental plants *indica* HJX74 and *japonica* IRAP9. *P*-values were generated from two-sided Student's *t* tests. Data are mean ± SEM (*n* = 6). (B) QTL analysis of a set of 71 SSSLs, each containing a single IRAP9 chromosomal segment in the HJX74 background. The positions of the two major QTLs are shown. (C) Genotyping of progeny homozygous for *qDNR1* delimited the locus to ∼132-kb stretch defined by the markers R15 and STS-1-20.2. Chromosomal segments homozygous for IRAP9 and HJX74 alleles are represented by filled and open bars, respectively. (D) $^{15}NO_3^-$ uptake rates for the 16 SSSLs. $^{15}NO_3^-$ uptake rate of HJX74 served as a control. Different letters denote significant differences (*P* < 0.05) from Duncan's multiple range test. Data are mean ± SEM (*n* = 6). (E) Morphology of mature NIL plants. Scale bar, 15 cm. (F) *DNR1* transcript abundance in roots. Transcript abundance was measured relative to NIL-*DNR1*^{HJX74} (set to 1). *P*-values were generated from two-sided Student's *t* tests. Data are mean ± SEM (*n* = 3). (G) DNR1 protein abundance in roots. The two DNR1 bands represent proteins encoded by two different *DNR1* transcripts, one encoding a protein containing 394 amino acids and the other encoding a C-terminally truncated protein with 208 amino acids. Data are representative of three independent experiments, with similar results. (H) Auxin content in roots. *P*-values were generated from two-sided Student's *t* tests. Data are mean ± SEM (*n* = 3). (I) Trp content in roots. *P*-values were generated from two-sided Student's *t* tests. Data are mean ± SEM (*n* = 3). (J) $^{15}NO_3^-$ uptake rate in roots. *P*-values were generated from two-sided Student's *t* tests. Data are mean ± SEM (*n* = 6). (K) *DNR1* mRNA levels in plants supplied with increasing levels of N (0.15 N, 0.1875 mM NH_4NO_3; 0.3 N, 0.375 mM NH_4NO_3; 0.6 N, 0.75 mM NH_4NO_3; 1 N, 1.25 mM NH_4NO_3). Transcript abundance was measured relative to 1N (set to 1). Different letters denote significant differences (*P* < 0.05) from Duncan's multiple range test. Data are mean ± SEM (*n* = 3). (L) DNR1 protein abundance in response to increasing N supply. The two DNR1 bands represent proteins encoded by two different *DNR1* transcripts, one encoding a protein containing 394 amino acids and the other encoding a C-terminally truncated protein with 208 amino acids. Data are representative of three independent experiments, with similar results.

increased abundance of *DNR1* mRNA and DNR1 protein compared to NIL-*DNR1*^HJX74 (Figure 1, F and G; Supplemental Figure S5, A–G). In addition, NIL-*DNR1*^IRAP9 plants had a relatively low auxin content but high Trp content, which is consistent with the predicted function of DNR1 (Figure 1, H and I). NIL-*DNR1*^IRAP9 plants also exhibited reduced NO_3^- uptake and reduced NR activity (Figure 1J; Supplemental Figure S5H). These results indicate that *DNR1*^indica is a reduced function allele conferring agronomically desirable traits. We examined the expression pattern of *DNR1* by quantitative polymerase chain reaction with reverse transcription (RT-qPCR) and found that it is mainly expressed in root, leaf, and node tissues (Supplemental Figure S4D). This expression pattern is consistent with the abovementioned phenotypic changes in NIL-*DNR1*^IRAP9 with regard to both root NO_3^- uptake and shoot architecture. Moreover, in addition to regulating NO_3^- uptake and reduction, we discovered that *DNR1* is regulated by N: the transcript level of *DNR1* increased with increasing N supply, which led to increased DNR1 protein abundance (Figure 1, K and L).

DNR1-mediated auxin homeostasis regulates N metabolism

To further explore the phenotypic consequences of varying *DNR1* expression and therefore auxin concentration in rice, we constructed *pAct:DNR1-Flag* overexpression lines and *dnr1* mutants in the Zhonghua 11 (ZH11; a *japonica* rice variety) background (Figure 2A; Supplemental Figure S6). The *dnr1* mutation was generated by clustered regularly interspaced short palindromic repeats (CRISPR)/CRISPR-associated protein 9 (Cas9), which resulted in a 2-bp deletion in the second exon of *DNR1* and therefore likely disrupts its normal gene function (Supplemental Figure S6, C and D). Notably, *dnr1* plants exhibited a tall stature, reduced tiller number, and increased IAA but reduced Trp content, whereas the opposite phenotypes were observed in *pAct:DNR1-Flag* overexpression lines (Figure 2, B–E).

We also examined whether altered *DNR1* levels lead to changes in root architecture. Compared to ZH11 and *dnr1*, the overexpression of *DNR1* repressed lateral root initiation and proliferation (Supplemental Figure S7). These results suggest that the upregulation of *DNR1* reduces root auxin contents, leading to a reduction in the size and production of lateral roots (Figure 2D; Supplemental Figure S7). Importantly, the lack of *DNR1* promoted both NO_3^- uptake and NR activity compared to ZH11, whereas plants overexpressing *DNR1* exhibited the lowest NO_3^- metabolic activities (Figure 2, F and G). The repressive effects of *DNR1* overexpression on NO_3^- metabolism was reversed by exogenous IAA treatment, which increased both the NO_3^- uptake rate and downstream NR activity to a level similar to those in ZH11, *pAct:DNR1-Flag* overexpression lines, and *dnr1* mutants (Figure 2, F and G). Taken together, these results confirm the notion that *DNR1*-mediated changes in auxin content affect plant growth and N metabolism.

To unravel the underlying mechanism of how *DNR1* and auxin modulate NO_3^- metabolism, we compared the transcript abundance of mRNAs encoding NO_3^- uptake transporters (e.g. *OsNRT1.1B*, *OsNRT2.3a*, and *OsNPF2.4*) and downstream NO_3^- assimilation enzymes (e.g. *OsNIA2*) by RT-qPCR. The expression levels of *OsNRT1.1B*, *OsNRT2.3a*, *OsNPF2.4*, and *OsNIA2* were higher in the *dnr1* mutants and lower in the *pAct:DNR1-Flag* overexpression lines compared to wild-type ZH11 (Figure 2, H–K). Therefore, DNR1 reduces auxin contents in rice, thereby repressing NUE by downregulating genes involved in NO_3^- metabolism.

OsARFs mediate the promotion of N metabolism by auxin

ARFs are a family of transcription factors that regulate the expression of auxin-responsive genes in a partially distinct manner (Li et al., 2016). In this study, RT-qPCR analyses identified seven *OsARF* members (*OsARF1*, *OsARF5*, *OsARF6*, *OsARF17*, *OsARF19*, *OsARF24*, and *OsARF25*) that were upregulated in *dnr1* but downregulated in *pAct:DNR1-Flag* overexpression plants compared to ZH11, as well as being repressed by high N supply (Supplemental Figure S8). We thus speculated that DNR1 modulates plant N metabolism via these key auxin signaling components. To test this hypothesis, we generated single knock-out mutants for these *OsARFs* using CRISPR/Cas9 in the ZH11 background (Supplemental Data Set 2) and measured their $^{15}NO_3^-$ uptake rates. Compared to the wild-type ZH11 control, the majority of the *osarf* mutations compromised $^{15}NO_3^-$ uptake capacity to various extents, suggesting that these OsARFs are involved in regulating NO_3^- uptake in rice (Figure 3A).

We selected *osarf6* and *osarf17*, whose $^{15}NO_3^-$ uptake rates were most affected, for further analysis. Both *osarf6* and *osarf17* mutants displayed a dwarf stature and enhanced tillering compared to ZH11 (Figure 3, B–D). These phenotypes are consistent with the phenotypes observed in the *DNR1* overexpression lines and in partially auxin-deficient plants. To confirm the regulatory effects of DNR1 and OsARFs on rice tillering, we compared the transcript levels of several known N-responsive regulators of tillering (*OsSPL14*, *D3*, *OsTB1*, and *D14* as repressors and *NGR5* as a promoter of tillering) in wild-type and the corresponding mutant plants (Takeda et al., 2003; Ishikawa et al., 2005; Arite et al., 2009; Jiao et al., 2010; Miura et al., 2010; Jiang et al., 2013; Zhou et al., 2013; Wang et al., 2017). Compared to ZH11, the expression levels of *OsSPL14*, *D3*, and *OsTB1* were reduced by *DNR1* overexpression and by the *osarf6* or *osarf17* loss-of-function mutations but increased in the *dnr1* mutant. No significant changes in *D14* or *NGR5* transcript abundance were detected in these plants (Supplemental Figure S9). Therefore, the enhanced tillering observed in *DNR1* overexpression, *osarf6*, and *osarf17* plants is likely caused by the inhibition of tillering repressors *OsSPL14*, *D3*, and *OsTB1*.

RT-qPCR assays demonstrated that *OsNRT1.1B*, *OsNRT2.3a*, *OsNPF2.4*, and *OsNIA2* mRNA levels were reduced in both *osarf6* and *osarf17* mutants, presumably due to a defective auxin signaling pathway (Figure 3, E–H). ARF transcription factors recognize and bind to TGTCTC/GAGACA sites
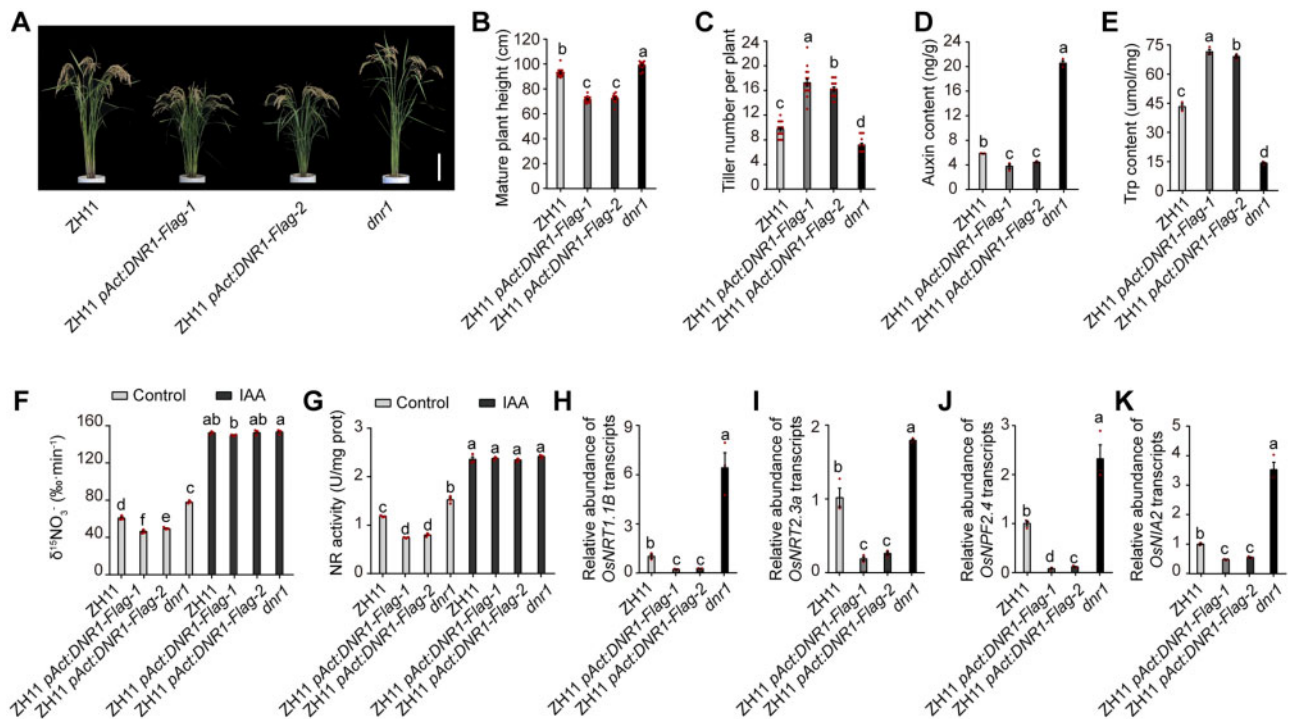
Figure 2 DNR1 regulates NO_3^- uptake and assimilation by modulating plant auxin level. (A) Morphology of mature ZH11, ZH11 *pAct:DNR1-Flag-1*, ZH11 *pAct:DNR1-Flag-2*, and *dnr1* plants. Scale bar, 20 cm. (B, C) Plant height (B) and number of tillers per plant (C) of ZH11, ZH11 *pAct:DNR1-Flag-1*, ZH11 *pAct:DNR1-Flag-2*, and *dnr1* plants. Data are mean ± SEM (n = 16). (D, E) Auxin content (D), and Trp content (E) in the roots of ZH11, ZH11 *pAct:DNR1-Flag-1*, ZH11 *pAct:DNR1-Flag-2*, and *dnr1* plants. Data are mean ± SEM (n = 3). (F, G) $^{15}NO_3^-$ uptake rate (F) and NR activities (G) of ZH11, ZH11 *pAct:DNR1-Flag-1*, ZH11 *pAct:DNR1-Flag-2*, and *dnr1* plants under mock and external IAA treatments (1 μM). Data are mean ± SEM (n = 3). H, I, mRNA abundances of *OsNRT1.1B* (H) and *OsNRT2.3a* (I) in roots relative to ZH11 (set to 1). Data are mean ± SEM (n = 3). (J, K) mRNA abundances of *OsNPF2.4* (J) and *OsNIA2* (K) in shoots relative to ZH11 (set to 1). Data are mean ± SEM (n = 3). (B–K) Different letters denote significant differences (P < 0.05) from Duncan's multiple range test.

through their highly conserved B$_3$-type DNA-binding domain (Kim et al., 1997; Tiwari et al., 2003; Piya et al., 2014; Chandler, 2016). Accordingly, chromatin-immunoprecipitation qPCR (ChIP-qPCR) and electrophoretic mobility shift assays (EMSAs) confirmed that both OsARF6 and OsARF17 bind directly to the TGTCTC/GAGACA-containing segments within the promoter regions of genes involved in NO_3^- uptake and assimilation (Figure 3, I and J; Supplemental Figures S10 and S11). Consequently, OsARF6 and OsARF17 activated transcription from the *OsNRT1.1B*, *OsNRT2.3a*, *OsNPF2.4*, and *OsNIA2* promoters in transient transactivation assays performed in rice protoplasts (Figure 3, K–N).

Next, we investigated whether exogenous IAA application would enhance NO_3^- uptake through OsARFs (Figure 4A). *OsARF6*, *OsARF17*, and NO_3^- metabolism-related genes (*OsNRT1.1B*, *OsNRT2.3a*, *OsNPF2.4*, and *OsNIA2*) were upregulated by IAA treatment (Figure 4, B–D). Specifically, IAA promoted ChIP-qPCR enrichment of TGTCTC/GAGACA motif-containing fragments from the *OsNRT1.1B* promoter, resulting in its elevated transcriptional activation compared to mock treatment (Figure 4, E and F; Supplemental Figure S12). Accordingly, the inhibited NO_3^- uptake in *osarf6* and *osarf17* was partially reverted by exogenous IAA treatment (Figure 4G).

Furthermore, overexpression of *OsARF6* or *OsARF17* significantly restored the deficiency in NO_3^- absorption caused by *DNR1* overexpression, although not to the same level as ZH11 (Figure 4H). Taken together, these observations suggest that although OsARFs share a certain degree of functional redundancy, neither OsARF6 nor OsARF17 is dispensable for promoting NO_3^- uptake in rice.

Increased auxin content promotes NUE and grain yield

As mentioned above, among our collection of 14 *indica* and 12 *japonica* varieties, their *DNR1* alleles are characterized by the absence and presence of a 520-bp promoter segment, respectively, which contribute to their differences in *DNR1* transcript levels and NO_3^- uptake activity (Supplemental Figure S2). On closer inspection, we discovered that this indel is linked to 11 SNPs in the promoter region of this gene (Supplemental Data Set 3), which also differentiate the *indica* and *japonica DNR1* alleles. To investigate if this applies more broadly to other varieties of these two subspecies, we conducted a haplotype analysis of the *DNR1* promoter in 216 rice accessions (Yu et al., 2017) and detected three distinct haplotypes (Haplotype A: 144 *indica* varieties; Haplotype B-TEJ: 60 temperate *japonica* varieties; Haplotype B-TRJ: 12 tropical *japonica* varieties). It is worth noting that
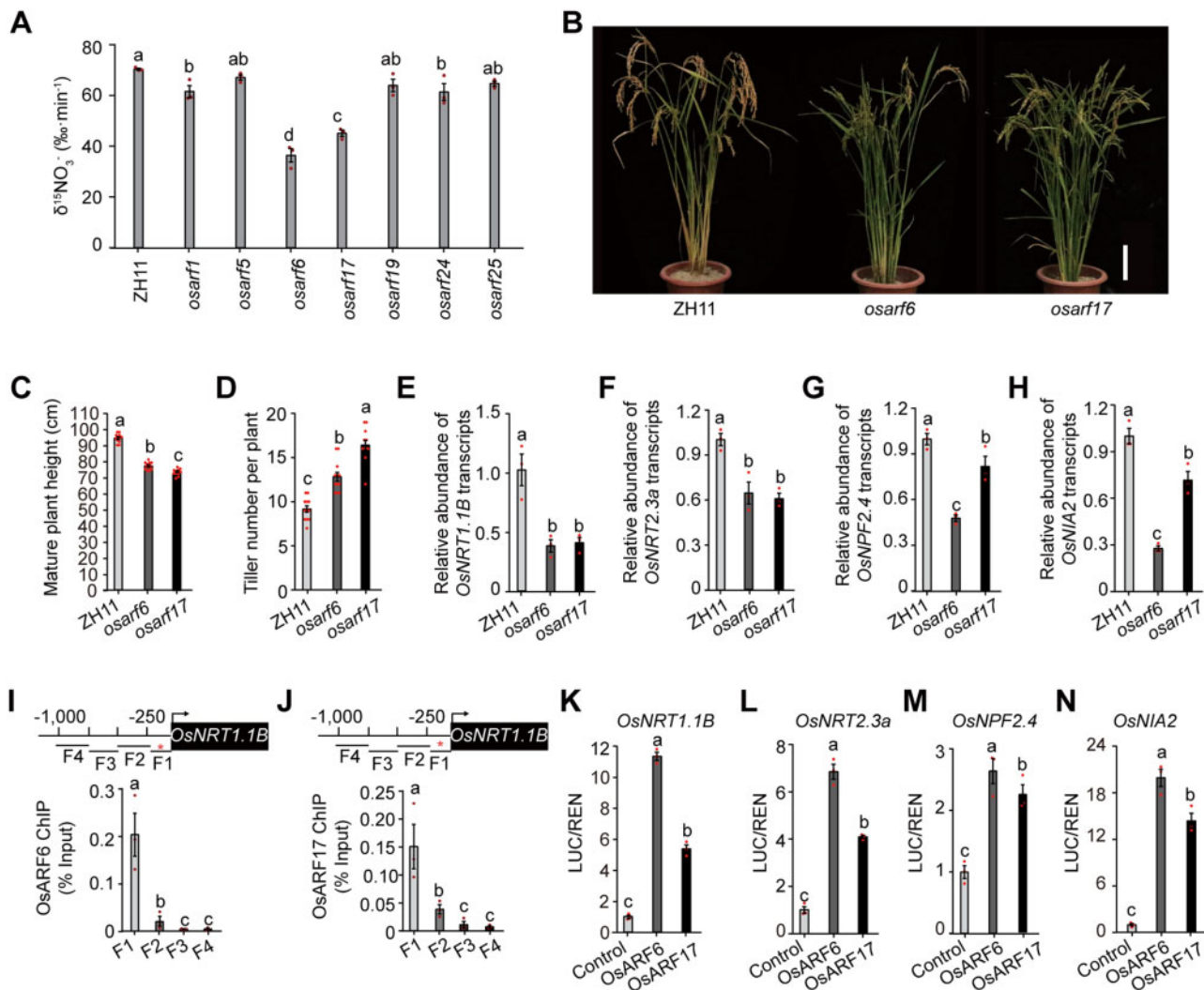
Figure 3 OsARFs regulate plant growth and promote the expression of multiple N-metabolism genes. (A) $^{15}NO_3^-$ uptake rate in roots of *osarf* mutants. Data are mean ± SEM (*n* = 3). (B) Morphology of mature ZH11, *osarf6*, and *osarf17* plants. Scale bar, 15 cm. (C, D) Plant height (C), and the number of tillers per plant (D) in ZH11, *osarf6*, and *osarf17* plants. Data are mean ± SEM (*n* = 12). (E, F) mRNA abundances of *OsNRT1.1B* (E) and *OsNRT2.3a* (F) in roots relative to ZH11 (set to 1). Data are mean ± SEM (*n* = 3). (G, H) mRNA abundances of *OsNPF2.4* (G) and *OsNIA2* (H) in shoots relative to ZH11 (set to 1). Data are mean ± SEM (*n* = 3). I, J, OsARF6-Flag and OsARF17-Flag-mediated ChIP-qPCR enrichment (relative to Input) of TGTCTC-containing promoter fragments (marked with an asterisk) from *OsNRT1.1B*. Data are mean ± SEM (*n* = 3). (K–N) OsARF6 and OsARF17 activate *OsNRT1.1B* (K), *OsNRT2.3a* (L), *OsNPF2.4* (M), and *OsNIA2* (N) promoter-LUC fusion constructs in transient transactivation assays. The LUC/REN activity obtained from a co-transfection with an empty effector construct and indicated reporter constructs was set to 1. Data are mean ± SEM (*n* = 3). (A, C–N) Different letters denote significant differences (*P* < 0.05) from Duncan's multiple range test.

haplotype A of the *DNR1* promoter contains the aforementioned 11 SNPs specific to *indica*. Furthermore, although haplotype A- and haplotype B-TEJ-containing varieties are commonly grown under similar planting conditions, Haplotype A is associated with increased plant height, reduced tillering, increased grain number, and higher grain yield potential, which is consistent with phenotypes caused by repressed *DNR1* expression and auxin accumulation (Figure 5).

Since we demonstrated that the relatively low *DNR1* transcript levels and the resulting high auxin levels in *indica* rice varieties promote N metabolism, we aimed to comprehensively examine the agronomic consequences of increasing

auxin content in the *japonica* ZH11 background by knocking out *DNR1*. Compared to ZH11 control plants, *dnr1* rice had enhanced NO_3^- metabolism, a taller stature, and lower tiller number under both high and low levels of N supply (Figure 6, A–E). Notably, although panicle primary branching was not detectably affected, grain yield per plant was promoted in the *dnr1* mutants, especially under lower levels of N supply, due to increases in the number of secondary branches and grains per panicle (Figure 6, F–I). This is likely due to the greater NO_3^- uptake and assimilation capacities exhibited by *dnr1*, which is evident from the higher total above-ground N content in the *dnr1* mutants relative to ZH11 (Supplemental Figure S13A). Nevertheless, the
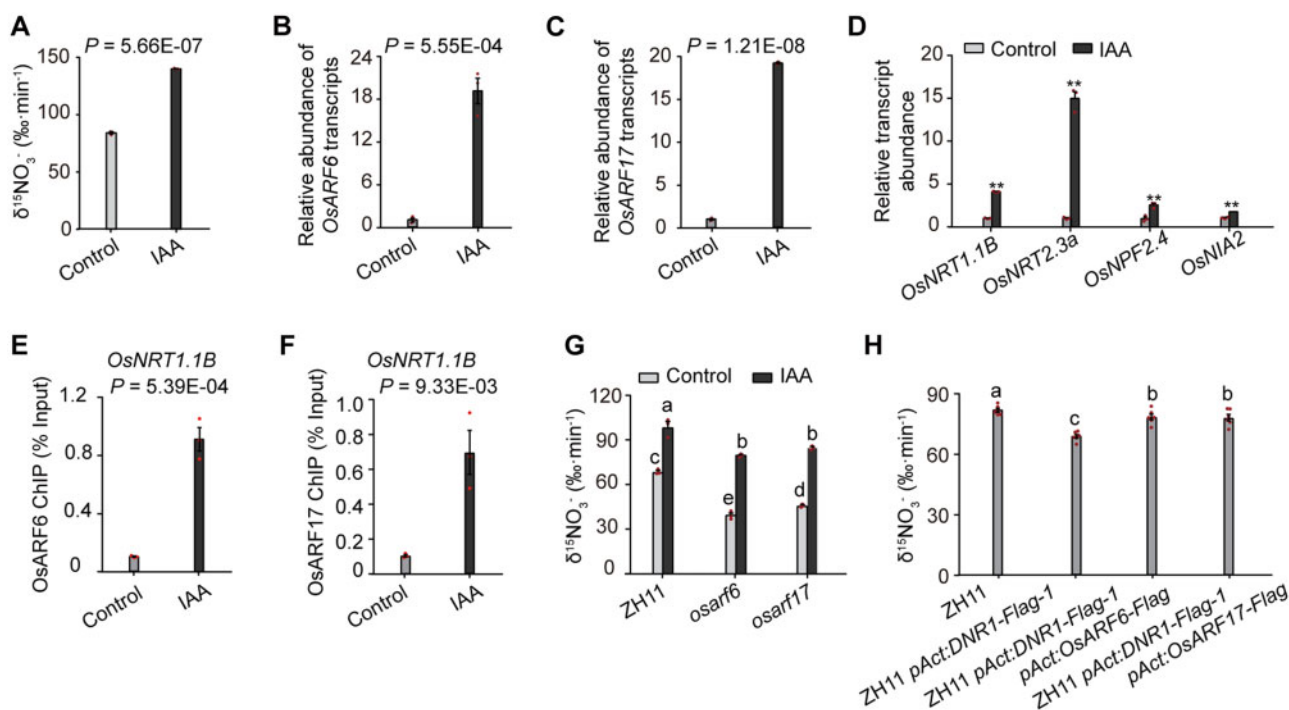
Figure 4 Auxin promotes the expression of N metabolism-related genes, and NO_3^- uptake is mediated by OsARFs. (A) $^{15}NO_3^-$ uptake rate in the roots of two-week-old plants under mock and external IAA treatment (1 μM). *P*-values were generated from two-sided Student's *t* tests. Data are mean ± SEM (*n* = 3). (B, C) mRNA abundance of *OsARF6* and *OsARF17* in roots under IAA treatment relative to the control (set to 1). *P*-values were generated from two-sided Student's *t* tests. Data are mean ± SEM (*n* = 3). (D) mRNA abundance in roots and shoots under IAA treatment relative to the control (set to 1). ** indicates the least significant difference at 0.01 probability level, generated from Student's *t* tests. Data are mean ± SEM (*n* = 3). (E, F) Extent of OsARF6 and OsARF17-mediated ChIP-qPCR enrichment (relative to Input) of TGTCTC-containing promoter fragments from *OsNRT1.1B* (fragment 1; shown in Figure 3, I and J). *P*-values were generated from two-sided Student's *t*-tests. Data are mean ± SEM (*n* = 3). (G) $^{15}NO_3^-$ uptake rate in the roots of ZH11, *osarf6*, and *osarf17* plants under mock and external IAA treatment (1 μM). Different letters denote significant differences (*P* < 0.05) from Duncan's multiple range test. Data are mean ± SEM (*n* = 3). (H) $^{15}NO_3^-$ uptake rate in the roots of *OsARF6* and *OsARF17* overexpression lines in the ZH11 *pAct:DNR1-Flag-1* background. Different letters denote significant differences (*P* < 0.05) from Duncan's multiple range test. Data are mean ± SEM (*n* = 6).

distribution ratio of N in the four above-ground tissues examined (Brown rice; Husk, Rachis, and Peduncle; Leaves; Culm) was not significantly altered by the lack of *DNR1* (Supplemental Figure S13B).

In conclusion, our results collectively suggest that the difference in auxin content in *indica* and *japonica* rice varieties controlled by their respective *DNR1* variant alleles contributes to their differences in NUE and yield (Figure 7). Thus, manipulating auxin content via *DNR1* represents a promising strategy for sustainably increasing grain yield while reducing environmentally degrading levels of agricultural N input in rice.

Discussion

Current global crop productivity is governed by the excessive use of nitrogenous fertilizers, which have detrimental effects on both the environment and human health (Chen et al., 2014). Therefore, developing new crop varieties with high yields under low N conditions would be highly desirable in the near future. To achieve this goal, we need to understand the complex regulatory network controlling plant N metabolism. Increasing evidence suggests that external N

status affects the biosynthetic and signal transduction pathways of auxin, although little is known about the identities of the genes that are N-responsive and whether they, in turn, regulate N metabolism. In this study, we discovered and characterized *DNR1*, a regulator of NUE in rice, expanding the current knowledge of the crosstalk between auxin signaling and N metabolism.

We identified *qDNR1* as an important QTL for NO_3^- uptake in rice. This gene encodes an enzyme responsible for maintaining auxin homeostasis. The *DNR1* locus diverges in DNA sequence between *indica* and *japonica* rice subspecies. The lack of a 520-bp promoter segment of *DNR1*^{indica} results in lower DNR1 protein abundance, increased auxin content, and higher NO_3^- uptake in *indica* compared to *japonica* varieties (Figure 1; Supplemental Figures S1 and S2). Furthermore, a loss-of-function *dnr1* mutation confers auxin overaccumulation and enhances NO_3^- metabolism by upregulating genes encoding NO_3^- transporters and NR (Figure 2). Notably, *DNR1* transcript abundance is induced by N, therefore forming a negative feedback regulatory loop (Figure 1, K and L). Taken together, we demonstrated that DNR1 functions as a mediator of plant N metabolism by
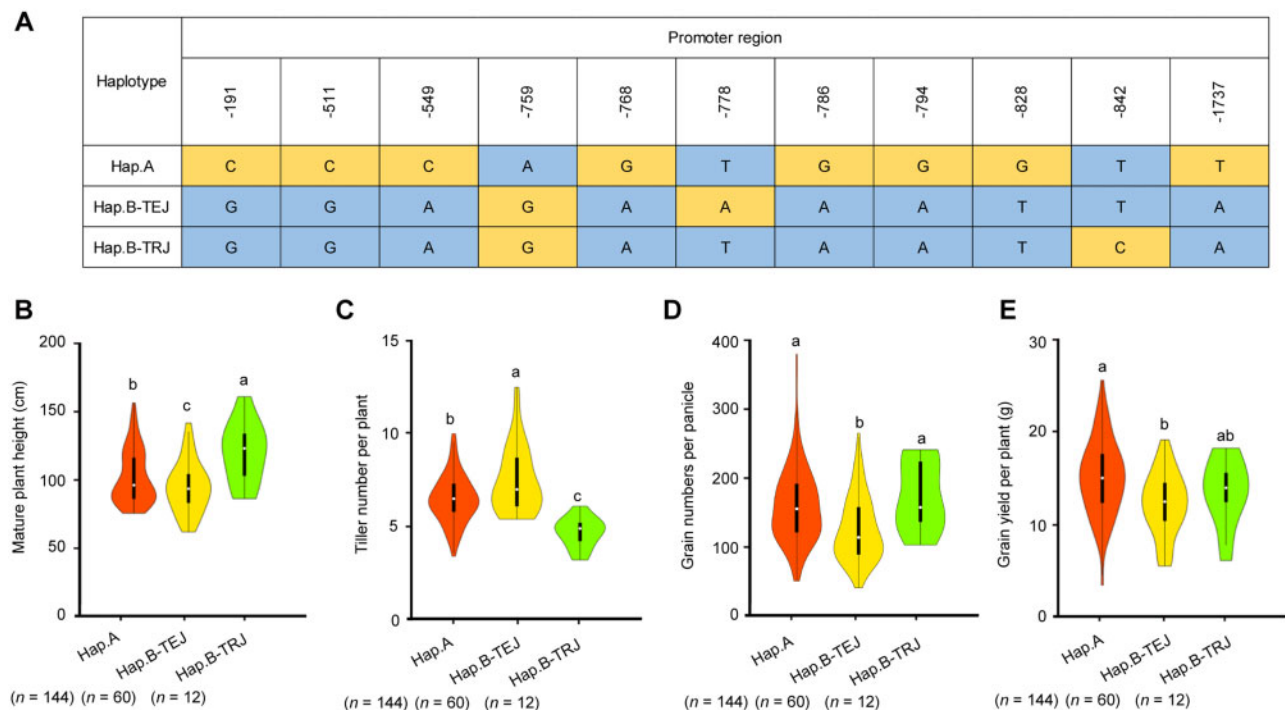
Figure 5 Natural allelic variation of DNR1 is associated with variation in plant and grain morphology and grain yield performance. (A) DNA polymorphisms in the promoter region of *DNR1*. (B–E) Violin plots for plant height (B), number of tillers per plant (C), number of grains per panicle (D), and grain yield (E) of rice varieties carrying different *DNR1* promoter haplotypes (Haplotype A, Haplotype B-TEJ, or Haplotype B-TRJ). All data are from plants grown under normal paddy-field fertilization conditions. Data are mean ± SEM (Haplotype A, $n = 144$; Haplotype B-TEJ, $n = 60$; Haplotype B-TRJ, $n = 12$). Different letters indicate statistically significant differences between groups ($P < 0.05$) from Tukey's honestly significant difference test.

antagonizing auxin accumulation and is itself regulated by N availability.

ARF family transcription factors play key roles in relaying auxin signals to alter plant growth and developmental processes. ARF8 is essential for mediating normal root developmental responses to external N in Arabidopsis (Wu et al., 2006). Interestingly, we showed that in rice, auxin-mediated promotion of NO_3^- uptake is also controlled by members of the *OsARF* family, since some *osarf* mutations, especially *osarf6* and *osarf17*, lead to significantly reduced NO_3^- uptake rates. We confirmed that OsARF6 and OsARF17, which belong to the same subclass as Arabidopsis ARF8 (Wang et al., 2007), act as transactivators of N metabolism-related genes by directly binding to the TGTCTC/GAGACA-containing segments within their promoter regions (Figure 3; Supplemental Figures S10 and S11). Accordingly, the overexpression of *OsARF6* or *OsARF17* counteracted the repressive activity of DNR1 on NO_3^- uptake (Figure 4H). However, this restoration was incomplete in both cases, and exogenous IAA treatment only partially recovered the NO_3^- uptake rates of *osarf6* and *osarf17* mutants (Figure 4G). These results suggest that OsARF6 and OsARF17 synergistically promote NO_3^- metabolism and that the NO_3^- uptake rate in a rice mutant lacking both *OsARF6* and *OsARF17* might have a strongly reduced response to auxin.

Members of the ARF family can be divided into transcriptional activators and repressors, depending on the amino acid composition of the nonconserved middle region subdomain; both OsARF6 and OsARF17 are categorized as transcriptional activators (Shen et al., 2010). However, our mutant analysis indicated that a number of OsARFs, including both transcriptional activators (OsARF5, OsARF6, OsARF17, OsARF19, and OsARF25) and repressors (OsARF1 and OsARF24), are positive regulators of NO_3^- uptake in roots (Figure 3A). For example, *OsNRT1.1B*, *OsNRT2.3a*, *OsNPF2.4*, and *OsNIA2* transcript levels were slightly reduced in the rice *osarf1* and *osarf24* mutants compared to the wild-type (Supplemental Figure S14). Further investigations are therefore needed to resolve whether some OsARFs, especially those belonging to the transcriptional repressor category, activate NO_3^- uptake through a distinct molecular mechanism.

Finally, we constructed *dnr1* mutant lines in the *japonica* ZH11 background, which mimic the generally lower *DNR1* transcript levels caused by the *DNR1^indica* allele in *indica* rice varieties, and investigated their agronomic traits. Briefly, the above-ground architecture was moderately altered by the *dnr1* mutation due to increased auxin accumulation, but crucially, both NUE and grain yield were significantly enhanced in the mutant lines compared to ZH11, without detectably affecting N distribution (Figure 6; Supplemental
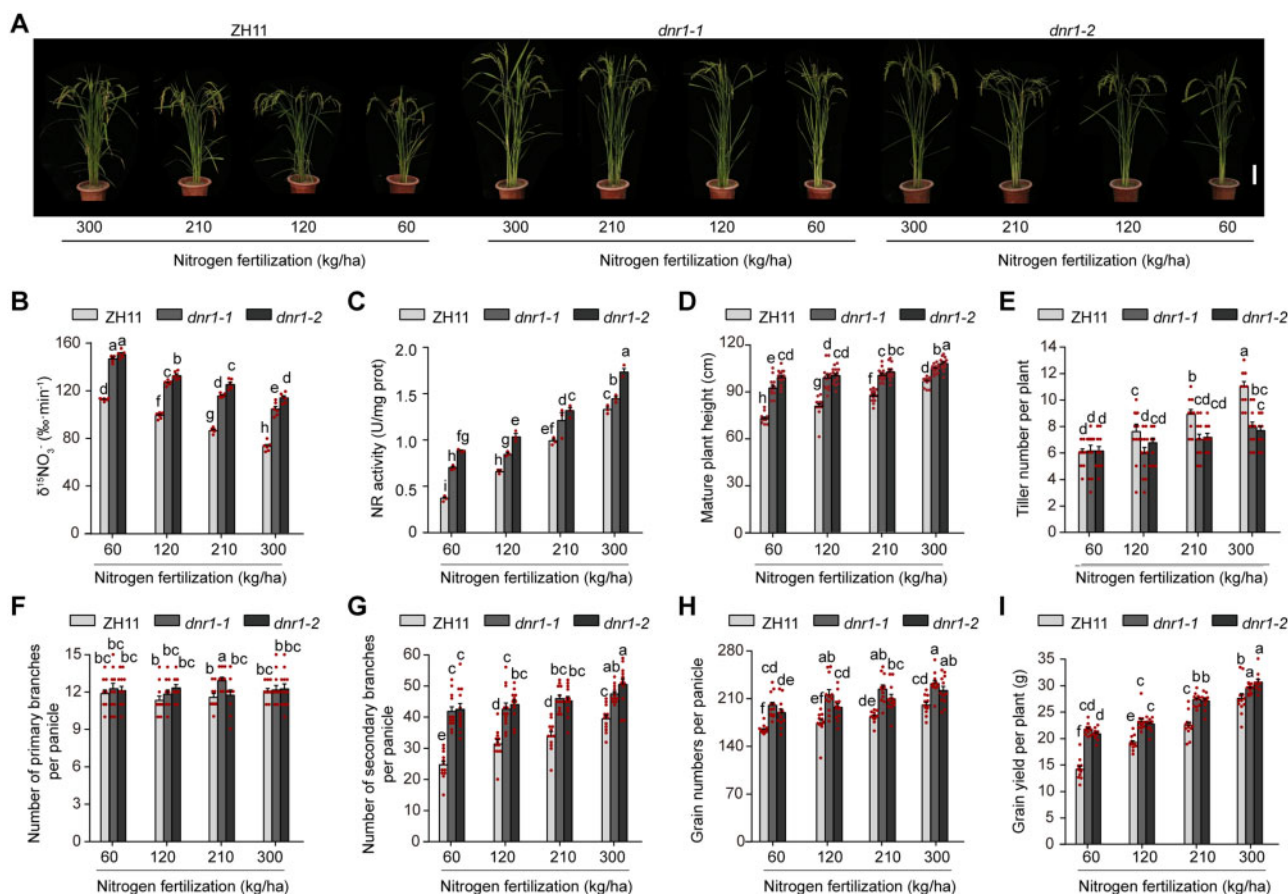
Figure 6 *dnr1* mutants have increased grain yield and NUE. (A) Morphology of mature ZH11, *dnr1-1*, and *dnr1-2* plants supplied with different levels of N. Scale bar, 15 cm. (B) $^{15}NO_3^-$ uptake rate in roots. Data are mean ± SEM ($n = 6$). (C) NR activity. Data are mean ± SEM ($n = 3$). (D) Plant height. Data are mean ± SEM ($n = 16$). (E–I) Number of tillers per plant (E), number of primary branches per plant (F), number of secondary branches per plant (G), number of grains per panicle (H), and grain yield per plant (I) of ZH11, *dnr1-1*, and *dnr1-2* plants. Data are mean ± SEM ($n = 12$). (B–I) Different letters denote significant differences ($P < 0.05$) from Duncan's multiple range test.

Figure S13). Therefore, we propose that the DNR1-Auxin-OsARFs cascade represents an important target that could be exploited to enhance crop NUE, thereby facilitating sustainable farming in the future (Figure 7).

Materials and methods

Plant materials and growth conditions in the field

Detailed information about the rice (*O. sativa*) germplasm used in this study for positional cloning and haplotype analysis was reported previously (Sun et al., 2014; Wang et al., 2017; Yu et al., 2017; Li et al., 2018). A set of 71 SSSLs were derived from a cross between HJX74 (an elite *indica* variety from South China) as the recipient parent and IRAP9 (a *japonica* variety from Brazil) as the donor parent. Each SSSL contains a single substituted segment from IRAP9 in the HJX74 genetic background, which was used for QTL analysis and map-based cloning. NIL-*DNR1*^{IRAP9} plants were generated by crossing the HJX74 × 27-055 F$_1$ hybrid with HJX74 (the recurrent parent) at least 6 times. Field-grown rice plants were raised under standard paddy conditions at experimental stations in Lingshui (Hainan Province) and

Hefei (Anhui Province), China, as previously described (Sun et al., 2014; Li et al., 2018;). Phenotypic parameters of rice, such as plant height, tiller number per plant, and grain yield per plant, were measured as previously described (Hu et al., 2015a, 2015b).

Hydroponic culture of plants

Seeds were sterilized with 20% NaClO solution for 30 min, and uniformly growing individuals after germination were selected for further analyses as described previously (Li et al., 2018). Seven-day-old seedlings were transferred to 40 L of nutrient solution (1.25 mM NH$_4$NO$_3$, 0.3 mM NaH$_2$PO$_4$·2H$_2$O, 0.35 mM K$_2$SO$_4$, 1 mM CaCl$_2$, 1 mM MgSO$_4$·7H$_2$O, 20 μM EDTA (ethylenediaminetetraacetic acid)–Fe, 0.5 mM Na$_2$SiO$_3$, 9 μM MnCl$_2$, 20 μM H$_3$BO$_3$, 0.77 μM ZnSO$_4$, 0.32 μM CuSO$_4$, and 0.39 μM (NH$_4$)$_6$Mo$_7$O$_{24}$, pH 5.5) in PVC (polyvinyl chloride) pots and grown for 4 weeks. When required, N concentrations were varied by replacing 1.25 mM NH$_4$NO$_3$ (1 N) with 0.75 mM NH$_4$NO$_3$ (0.6 N), 0.375 mM NH$_4$NO$_3$ (0.3 N), or 0.1875 mM NH$_4$NO$_3$ (0.15 N). All nutrient solutions were replaced twice per week, and the pH was adjusted to 5.5
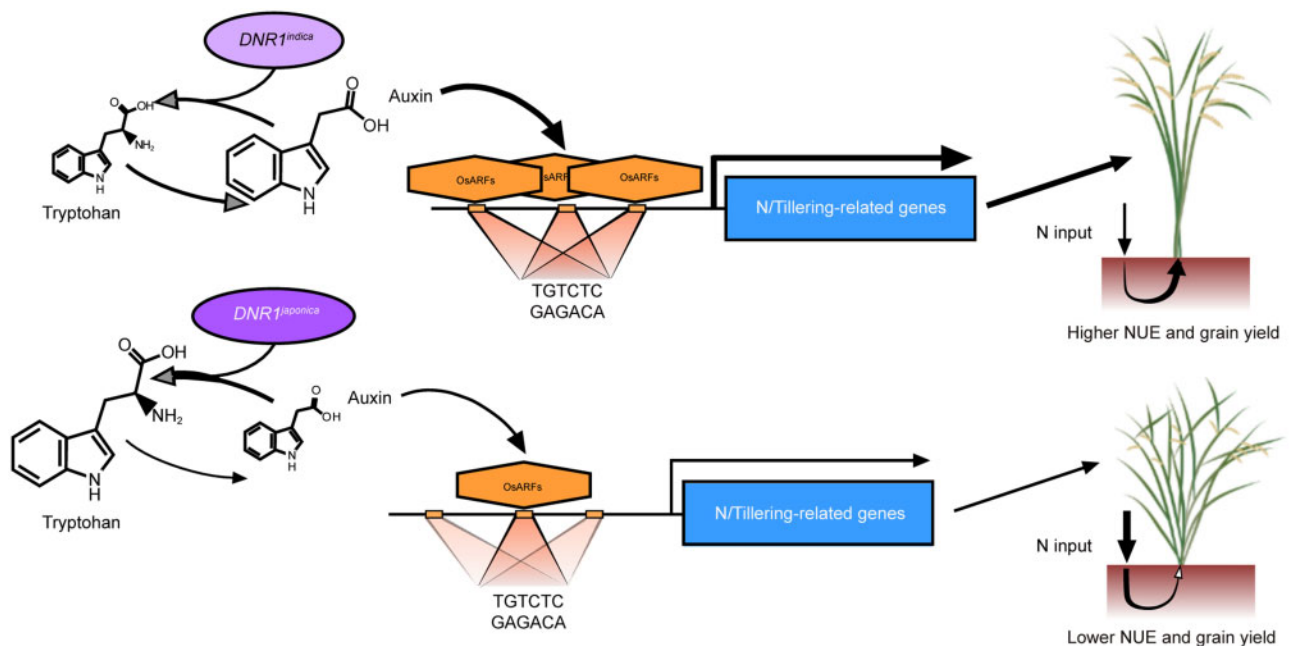
Figure 7 Model of how rice NUE and yield are regulated by the DNR1–auxin–OsARFs module in *indica* and *japonica* rice varieties. The $DNR1^{indica}$ variant allele leads to reduced transcript and protein abundances of DNR1, and therefore the accumulation of auxin. This consequently induces OsARF-mediated activation of genes involved in both N metabolism and the inhibition of tillering. As a result, rice plants carrying the $DNR1^{indica}$ allele exhibit high yield with reduced N requirement. On the contrary, the $DNR1^{japonica}$ allele confers increased tillering and N demand due to a reduced auxin level.

daily. The temperature was maintained at 16 h light (30°C) and 8 h dark (22°C) with an ~400 μmol/s/m^2 photon density and a relative humidity of 60%.

QTL analysis and fine mapping of *DNR1*
Seventy-one SSSLs were used for QTL analysis, from which two main QTLs for NO_3^- uptake were identified. One hundred and forty-four BC_1F_2 and 947 BC_2F_2, derived from 27-055 and HJX74, were used for fine mapping. The primer sequences used for map-based cloning and genotyping assays are listed in Supplemental Data Set 1.

Phylogenetic analysis
The amino acid sequences of DNR1 and its homologs in other plants (15 amino acid sequences) were downloaded from PLAZA (https://bioinformatics.psb.ugent.be/plaza/) and are provided in Supplemental File 1. Phylogenetic analyses were carried out in MEGA7 (Kumar et al., 2016), and the phylogenetic tree was constructed using the Neighbor-Joining method (500-bp replications; Felsenstein, 1985). The evolutionary distances were calculated using the Poisson correction method and represent the number of amino acid substitutions per site. After discarding all ambiguous positions for each sequence pair, 548 positions were included in the final dataset.

Transgene constructs
The full-length *DNR1*, *OsARF6*, and *OsARF17* cDNAs were amplified from ZH11 before being inserted into *pAct:Flag-nos* using Gateway recombination cloning technology

according to the manufacturer's instructions (Invitrogen, Carlsbad, CA, USA; 11789100 and 11791100) , to generate the *pAct:DNR1-Flag*, *pAct:OsARF6-Flag*, and *pAct:OsARF17-Flag* constructs. Similarly, full-length *DNR1* was inserted into *p35S:GFP-nos* to generate the *p35S:DNR1-GFP* construct (Wang et al., 2012). gRNA constructs used to produce the CRISPR/Cas9-generated *DNR1*, *OsARF1*, *OsARF5*, *OsARF6*, *OsARF17*, *OsARF19*, *OsARF24*, and *OsARF25* loss-of-function alleles in the ZH11 genetic background were generated as described elsewhere (He et al., 2018). Transgenic rice plants were generated by *Agrobacterium*-mediated transformation as described elsewhere (Huang et al., 2009). Target information for CRISPR/Cas9-generated mutants is listed in Supplemental Data Set 2. Relevant primer sequences are listed in Supplemental Data Set 4.

RT-qPCR analysis
Total RNAs were extracted from different plant tissues using TRIzol reagent (Ambion, Austin, TX, USA), and full-length cDNAs were reverse transcribed using a cDNA synthesis kit (Vazyme, Nanjing, China; R323-01). qPCR was performed on a CFX96 real-time PCR detection system (Bio-Rad, Hercules, CA, USA). Each reaction contained 5 μL diluted cDNA, 0.5-μL primers, and 10 μL SYBR Green Master Mix in a total volume of 20 μL, according to the manufacturer's instructions (Vazyme; Q111-02). The program included a melting step at 95°C for 30 s and an amplification step consisting of 40 cycles of 95°C for 5 s followed by 60°C for 20 s. All RT-qPCR experiments were performed with three biological replicates (obtained from independent extraction processes using

separate plant materials). The values of transcript abundance represent the average of three technical replicates (separate qPCRs using the same cDNA). The rice *ACTIN1* gene was used as an internal control. Relevant RT-qPCR primer sequences are listed in Supplemental Data Set 5.

Immunoblot analysis

Extraction buffer containing 50 mM Tris–HCl (pH 7.5), 150 mM NaCl, 0.1% NP-40 detergent, 10% glycerol, 1 mM DTT (dithiothreitol) and protease inhibitor cocktail (Roche LifeScience, Penzberg, Germany) was used to extract total protein. Protein samples were separated by 10% SDS–PAGE (sodium dodecyl sulphate-polyacrylamide gel electrophoresis) and transferred to a nitrocellulose membrane under wet transfer conditions. DNR1 protein was detected by probing the membrane with anti-DNR1 (ABclonal, Woburn, MA, USA) and anti-DDDDK-tag antibodies (MBL, Woburn, MA, USA, M185-11, and Lot.007). The results of immunoblotting were visualized on the Tanon-5200 Chemiluminescent Imaging System (Tanon Science and Technology).

Preparation of nuclear and cellular protein extracts

Extraction buffer containing Ficoll (25 mg/mL), Dextran T 40 (50 mg/mL), sucrose (137 mg/mL), 25 mM Tris–HCl (pH 7.4), 10 mM $MgCl_2$, 0.5 mM DTT, and protein inhibitor cocktail (Roche LifeScience) was used to separate cytoplasmic and nuclear proteins. The DNR1–GFP, GRF4-GFP, and free GFP proteins were detected by probing the membrane with anti-GFP antibody (MBL, 598-7, and Lot.005). The results of immunoblotting were visualized on the Tanon-5200 Chemiluminescent Imaging System (Tanon Science and Technology).

ChIP-qPCR assays

Details of ChIP-qPCR analysis have been described elsewhere (O'Geen et al., 2010). Briefly, ~2 g samples of 2-week-old wild-type and transgenic rice seedlings (*pAct:OsARF6-Flag* and *pAct:OsARF17-Flag*) were fixed with 1% formaldehyde, subjected to cross-linking under a vacuum for 15 min to cross-link protein–DNA complexes, and ground into a fine powder in liquid N. Following isolation and lysis of nuclei, chromatin was isolated and fragmented by ultrasonication into ~500-bp fragments. The sonicated chromatin was incubated with 7 µg of antibody-Flag (Sigma, St Louis, MO, USA; F1804) overnight at 4°C for immunoprecipitations. The next day, washing, elution, reverse cross-linking, and DNA purification steps were performed. Enrichment of DNA fragments was determined by RT-qPCR analysis performed on three biological replicates (obtained from independent extraction processes using separate plant materials). Relevant PCR primer sequences are listed in Supplemental Data Set 6.

EMSA

Full-length *OsAFR6* and *OsARF17* cDNAs were amplified and cloned into the pCold-TF vector (Takara, Kyoto, Japan). His-OsAFR6 and His-OsAFR17 recombinant proteins were purified using Ni-NTA agarose (Qiagen, Hilden, Germany; 30210) following the manufacturer's instructions. DNA probes were artificially amplified and labeled using a biotin label kit (Sangon Biotech, Shanghai, China). DNA gel shift assays were performed using a LightShift Chemiluminescent EMSA kit (Thermo Fisher Scientific, Waltham, MA, USA; 20148). Relevant primer sequences are listed in Supplemental Data Set 7.

In vitro transient transactivation assays

Approximately 2-kb DNA promoter fragments from *OsNRT1.1B*, *OsNRT2.3a*, *OsNPF2.4*, and *OsNIA2* were amplified from ZH11 and inserted into the *Eco*RV and *Xba*I sites of pUC19 containing the firefly luciferase (*LUC*) reporter gene driven by the 35S minimal TATA box and 5 × GAL4 binding elements. Full-length cDNAs of *OsARF6* and *OsARF17* were amplified and fused to the sequence encoding GAL4BD by inserting them into the BamHI and EcoRI sites of pRTBD to generate the effector plasmids *pRTBD-OsARF6* and *pRTBD-OsARF17*, respectively. Transient transactivation assays were performed using rice protoplasts as described elsewhere (Wang et al., 2015). The Dual-LUC Reporter Assay System (Promega, Madison, WI, USA; E1960) and the GloMax^TM 20-20 Luminometer were used for the LUC activity assays, with the *Renilla* (REN) *LUC* gene used as an internal control. Relevant PCR primer sequences are listed in Supplemental Data Set 4.

Determination of IAA content

Samples of ~50-mg root tip tissue were ground into a powder in liquid N and extracted with methanol/water/formic acid (15:4:1, V/V/V). The combined extracts were evaporated to dryness under an N-gas stream, reconstituted in 80% methanol (V/V), filtrated (PTFE, 0.22 µm, Anpel), and analyzed using an LC–ESI–MS/MS (liquid chromatography-electrospray ionization-tandem mass spectrometry) system and ESI-triple quadrupole-linear ion trap–MS system (Flokova et al., 2014; Cui et al., 2015; Simura et al., 2018; Xiao et al., 2018).

Determination of Trp content

Samples of ~25-mg plant tissue were treated with methanol/acetonitrile/water (2:2:1, V/V/V), ground into a powder, and ultrasonically cracked in an ice bath for 10 min (Power: 80 Hz). Following centrifugation for 15 min (25,000 g, 4°C), 500 µL of supernatant was freeze-dried. The drained supernatant was re-dissolved in 500 µL 10% methanol solution and analyzed using the LC–MS/MS Sciex5500-Transcend II system.

^{15}N uptake analysis

After growth in hydroponic culture for 4 weeks, $^{15}NO_3^-$ influx into roots was measured as described elsewhere (Ho et al., 2009; Li et al., 2018). Roots and shoots were separated, dried at 80°C for 72 h, and the ^{15}N content measured using the Isoprime 100 elemental analyzer (Elementar, Langenselbold, Germany).

Measurement of NR activity

Fresh plant material (~1 g) from individual rice plant supplied with four different N levels was used to measure NR

activity, following the instruction manual of the NR Kit (Solarbio LIFE SCIENCES, Beijing, China; BC0080).

Determination of plant N concentration

Samples from different plant organs were dried in an oven at 80°C for 72 h. Following tissue homogenization, N content was measured using an elemental analyzer (IsoPrime100; Elementar).

Accession numbers

Sequence data of the rice genes studied in this article can be found in The Rice Annotation Project Database (https://rapdb.dna.affrc.go.jp/) under the following accession numbers: DNR1 (LOC_Os01g08270), OsNRT1.1B (LOC_Os10g40600), OsNRT2.3a (LOC_Os01g50820), OsNPF2.4 (LOC_Os01g36720), OsNIA2 (LOC_Os08g36500), OsARF1 (LOC_Os01g13520), OsARF5 (LOC_Os02g04810), OsARF6 (LOC_Os02g06910), OsARF17 (LOC_Os06g46410), OsARF19 (LOC_Os06g48950), OsARF24 (LOC_Os12g29520), and OsARF25 (LOC_Os12g41950).

Supplemental data

The following materials are available in the online version of this article.

Supplemental Figure S1. Identification of DNR1 by fine-scale mapping, and sequence divergence in this gene between rice varieties HJX74 and IRAP9.

Supplemental Figure S2. The 520-bp INDEL in the DNR1 promoter underlies the differences in DNR1 transcript level and NO_3^- uptake rate between indica and japonica varieties.

Supplemental Figure S3. Phylogenetic tree of DNR1 and its homologous genes, and amino acid sequence alignment of DNR1 and Arabidopsis VAS1.

Supplemental Figure S4. Subcellular localization and expression pattern of DNR1.

Supplemental Figure S5. Shoot architecture and NR activity of mature NIL plants.

Supplemental Figure S6. DNR1 transcript abundance and DNR1 protein accumulation in ZH11 pAct:DNR1-Flag and dnr1 plants compared to ZH11.

Supplemental Figure S7. Reducing auxin contents by increasing DNR1 abundance disturbs lateral root development.

Supplemental Figure S8. The seven OsARFs whose transcript abundances are significantly increased in dnr1 plants.

Supplemental Figure S9. Transcript abundances of key regulators of tillering in ZH11, ZH11 pAct:DNR1-Flag, dnr1, osarf6, and osarf17 plants.

Supplemental Figure S10. OsARF-mediated ChIP-qPCR enrichment of TGTCTC-containing promoter fragments from genes involved in NO_3^- metabolism.

Supplemental Figure S11. His-OsARFs bind directly to the promoters of genes related to NO_3^- metabolism.

Supplemental Figure S12. Auxin promotes the transactivation of OsARF6 and OsARF17 toward OsNRT1.1B.

Supplemental Figure S13. N distributions in different organs of above-ground parts of ZH11 and dnr1 rice plants.

Supplemental Figure S14. Transcript abundances of N-related genes in ZH11, osarf1, and osarf24 plants.

Supplemental Data Set 1. Primer sequences used for map-based cloning and genotyping assays.

Supplemental Data Set 2. Information about osarf mutants.

Supplemental Data Set 3. SNPs in the OsDNR1 promoter region of indica and japonica rice varieties.

Supplemental Data Set 4. Primer sequences used for transgene construction.

Supplemental Data Set 5. Primer sequences used for qPCR assays.

Supplemental Data Set 6. Primer sequences used for ChIP assays.

Supplemental Data Set 7. Primer sequences used for EMSAs.

Supplemental File 1. Amino acid sequences of DNR1 and its homologs in other plants used for phylogenetic analysis.

References

Arite T, Umehara M, Ishikawa S, Hanada A, Maekawa M, Yamaguchi S, Kyozuka J (2009) d14, a strigolactone-insensitive mutant of rice, shows an accelerated outgrowth of tillers. Plant Cell Physiol **50**: 1416–1424

Avery GS, Burkholder PR, Creighton HB (1937) Nutrient deficiencies and growth hormone concentration in *Helianthus* and *Nicotiana*. Am J Bot **24**: 553–557

Avery GS, Pottorf L (1945) Auxin and nitrogen relationships in green plants. Am J Bot **32**: 666–669

Caba JM, Centeno ML, Fernández B, Gresshoff PM, Ligero F (2000) Inoculation and nitrate alter phytohormone levels in soybean roots: differences between a supernodulating mutant and the wild type. Planta **211**: 98–104

Chandler JW (2016) Auxin response factors. Plant Cell Environ **39**: 1014–1028

Che R, Tong H, Shi B, Liu Y, Fang S, Liu S, Liu D, Xiao Y, Hu B, Liu L et al. (2015) Control of grain size and rice yield by GL2-mediated brassinosteroid responses. Nat Plants **2:** 15195

Chen X, Cui Z, Fan M, Vitousek P, Zhao M, Ma W, Wang Z, Zhang W, Yan X, Yang J et al. (2014) Producing more grain with lower environmental costs. Nature **514:** 486–489

Chen ZC, Ma JF (2015) Improving nitrogen use efficiency in rice through enhancing root nitrate uptake mediated by a nitrate transporter, NRT1.1B. J Genet Genomics **42:** 463–465

Cui K, Lin Y, Zhou X, Li S, Liu H, Zeng F, Zhu F, Ouyang G, Zeng Z (2015) Comparison of sample pretreatment methods for the determination of multiple phytohormones in plant samples by liquid chromatography–electrospray ionization-tandem mass spectrometry. Microchem J **121:** 25–31

Duan D, Zhang H (2015) A single SNP in NRT1.1B has a major impact on nitrogen use efficiency in rice. Sci China Life Sci **58:** 827–828

Duan P, Shen N, Wang J, Zhang B, Xu R, Wang Y, Chen H, Zhu X, Li Y (2015) Regulation of OsGRF4 by osmiR396 controls grain size and yield in rice. Nat Plants **2:** 15203

Fan X, Feng H, Tan Y, Xu Y, Miao Q, Xu G (2016) A putative 6-transmembrane nitrate transporter OsNRT1.1b plays a key role in rice under low nitrogen. J Integr Plant Biol **58:** 590–599

Felsenstein J (1985) Confidence limits on phylogenies: an approach using the bootstrap. Evolution **39:** 783–791

Flokova K, Tarkowska D, Miersch O, Strnad M, Wasternack C, Novak O (2014) UHPLC-MS/MS based target profiling of stress-induced phytohormones. Phytochemistry **105:** 147–157

Gao Z, Wang Y, Chen G, Zhang A, Yang S, Shang L, Wang D, Ruan B, Liu C, Jiang H et al. (2019) The indica nitrate reductase gene OsNR2 allele enhances rice yield potential and nitrogen use efficiency. Nat Commun **10:** 5207

Gifford ML, Dean A, Gutierrez RA, Coruzzi GM, Birnbaum KD (2008) Cell-specific nitrogen responses mediate developmental plasticity. Proc Natl Acad Sci USA **105:** 803–808

Godfray HC, Beddington JR, Crute IR, Haddad L, Lawrence D, Muir JF, Pretty J, Robinson S, Thomas SM, Toulmin C (2010) Food security: the challenge of feeding 9 billion people. Science **327:** 812–818

Guo JH, Liu XJ, Zhang Y, Shen JL, Han WX, Zhang WF, Christie P, Goulding KW, Vitousek PM, Zhang FS (2010) Significant acidification in major Chinese croplands. Science **327:** 1008–1010

He Y, Zhu M, Wang L, Wu J, Wang Q, Wang R, Zhao Y (2018) Programmed self-elimination of the CRISPR/Cas9 construct greatly accelerates the isolation of edited and transgene-free rice plants. Mol Plant **11:** 1210–1213

Ho CH, Lin SH, Hu HC, Tsay YF (2009) CHL1 functions as a nitrate sensor in plants. Cell **138:** 1184–1194

Hu B, Wang W, Ou S, Tang J, Li H, Che R, Zhang Z, Chai X, Wang H, Wang Y et al. (2015a) Variation in NRT1.1B contributes to nitrate-use divergence between rice subspecies. Nat Genet **47:** 834–838

Hu J, Wang Y, Fang Y, Zeng L, Xu J, Yu H, Shi Z, Pan J, Zhang D et al. (2015b) A rare allele of GS2 enhances grain size and grain yield in rice. Mol Plant **8:** 1455–1465

Huang X, Qian Q, Liu Z, Sun H, He S, Luo D, Xia G, Chu C, Li J, Fu X (2009) Natural variation at the DEP1 locus enhances grain yield in rice. Nat Genet **41:** 494–497

Ishikawa S, Maekawa M, Arite T, Onishi K, Takamure I, Kyozuka J (2005) Suppression of tiller bud activity in tillering dwarf mutants of rice. Plant Cell Physiol **46:** 79–86

Jiang L, Liu X, Xiong G, Liu H, Chen F, Wang L, Meng X, Liu G, Yu H, Yuan Y et al. (2013). DWARF 53 acts as a repressor of strigolactone signalling in rice. Nature **504:** 401–405

Jiao Y, Wang Y, Xue D, Wang J, Yan M, Liu G, Dong G, Zeng D, Lu Z, Zhu X et al. (2010) Regulation of OsSPL14 by OsmiR156 defines ideal plant architecture in rice. Nat Genet **42:** 541–544

Kaiser J (2018) Too much of a good thing? Science **359:** 1346–1347

Kiba T, Kudo T, Kojima M, Sakakibara H (2011) Hormonal control of nitrogen acquisition: roles of auxin, abscisic acid, and cytokinin. J Exp Bot **62:** 1399–1409

Kim J, Harter K, Theologis A (1997) Protein-protein interactions among the Aux/IAA proteins. Proc Natl Acad Sci USA **94:** 11786–11791

Krouk G, Lacombe B, Bielach A, Perrine-Walker F, Malinska K, Mounier E, Hoyerova K, Tillard P, Leon S, Ljung K et al. (2010) Nitrate-regulated auxin transport by NRT1.1 defines a mechanism for nutrient sensing in plants. Dev Cell **18:** 927–937

Kumar S, Stecher G, Tamura K (2016) MEGA7: molecular evolutionary genetics analysis version 7.0 for bigger datasets. Mol Biol Evol **33:** 1870–1874

Li H, Hu B, Chu C (2017) Nitrogen use efficiency in crops: lessons from Arabidopsis and rice. J Exp Bot **68:** 2477–2488

Li S, Tian Y, Wu K, Ye Y, Yu J, Zhang J, Liu Q, Hu M, Li H, Tong Y et al. (2018) Modulating plant growth-metabolism coordination for sustainable agriculture. Nature **560:** 595–600

Li SB, Xie ZZ, Hu CG, Zhang JZ (2016) A review of auxin response factors (ARFs) in plants. Front Plant Sci **7:** 47

Li YL, Fan XR, Shen QR (2008) The relationship between rhizosphere nitrification and nitrogen-use efficiency in rice plants. Plant Cell Environ **31:** 73–85

Liu X, Zhang Y, Han W, Tang A, Shen J, Cui Z, Vitousek P, Erisman JW, Goulding K, Christie P et al. (2013) Enhanced nitrogen deposition over China. Nature **494:** 459–462

Luo L, Wang H, Liu X, Hu J, Zhu X, Pan S, Qin R, Wang Y, Zhao P, Fan X et al. (2018) Strigolactones affect the translocation of nitrogen in rice. Plant Sci **270:** 190–197

Luo L, Zhang Y, Xu G (2020) How does nitrogen shape plant architecture? J Exp Bot **71:** 4415–4427

Ma W, Li J, Qu B, He X, Zhao X, Li B, Fu X, Tong Y (2014) Auxin biosynthetic gene TAR2 is involved in low nitrogen-mediated reprogramming of root architecture in Arabidopsis. Plant J **78:** 70–79

Matsuo S, Miyatake K, Endo M, Urshimo S, Kawanishi T, Negoro S, Shimakoshi S, Fukuoka H (2020) Loss of function of the Pad-1 aminotransferase gene, which is involved in auxin homeostasis, induces parthenocarpy in Solanaceae plants. Proc Natl Acad Sci USA **117:** 12784–12790

Miura K, Ikeda M, Matsubara A, Song XJ, Ito M, Asano K, Matsuoka M, Kitano H, Ashikari M (2010) OsSPL14 promotes panicle branching and higher grain productivity in rice. Nat Genet **42:** 545–549

O'Geen H, Frietze S, Farnham PJ (2010) Using ChIP-seq technology to identify targets of zinc finger transcription factors. Methods Mol Biol **649:** 437–455

Pieck M, Yuan Y, Godfrey J, Fisher C, Zolj S, Vaughan D, Thomas N, Wu C, Ramos J, Lee N et al. (2015) Auxin and tryptophan homeostasis are facilitated by the ISS1/VAS1 aromatic aminotransferase in Arabidopsis. Genetics **201:** 185–199

Piya S, Shrestha SK, Binder B, Stewart CN, Jr, Hewezi T (2014) Protein-protein interaction and gene co-expression maps of ARFs and Aux/IAAs in Arabidopsis. Front Plant Sci **5:** 744

Sakakibara H, Takei K, Hirose N (2006) Interactions between nitrogen and cytokinin in the regulation of metabolism and development. Trends Plant Sci **11:** 440–448

Shen C, Wang S, Bai Y, Wu Y, Zhang S, Chen M, Guilfoyle TJ, Wu P, Qi Y (2010) Functional analysis of the structural domain of ARF proteins in rice (Oryza sativa L). J Exp Bot **61:** 3971–3981

Simura J, Antoniadi I, Siroka J, Tarkowska D, Strnad M, Ljung K, Novak O (2018) Plant hormonomics: multiple phytohormone profiling by targeted metabolomics. Plant Physiol **177:** 476–489

Sun H, Qian Q, Wu K, Luo J, Wang S, Zhang C, Ma Y, Liu Q, Huang X, Yuan Q et al. (2014) Heterotrimeric G proteins regulate nitrogen-use efficiency in rice. Nat Genet **46:** 652–656

Takeda T, Suwa Y, Suzuki M, Kitano H, Ueguchi-Tanaka M, Ashikari M, Matsuoka M, Ueguchi C (2003) The OsTB1 gene negatively regulates lateral branching in rice. Plant J **33:** 513–520

Tang W, Ye J, Yao X, Zhao P, Xuan W, Tian Y, Zhang Y, Xu S, An H, Chen G et al. (2019) Genome-wide associated study identifies NAC42-activated nitrate transporter conferring high nitrogen use efficiency in rice. Nat Commun 10: 5279

Tian Q, Chen F, Liu J, Zhang F, Mi G (2008) Inhibition of maize root growth by high nitrate supply is correlated with reduced IAA levels in roots. J Plant Physiol 165: 942–951

Tiwari SB, Hagen G, Guilfoyle T (2003) The roles of auxin response factor domains in auxin-responsive transcription. Plant Cell 15: 533–543

Vidal EA, Araus V, Lu C, Parry G, Green PJ, Coruzzi GM, Gutierrez RA (2010) Nitrate-responsive miR393/AFB3 regulatory module controls root system architecture in Arabidopsis thaliana. Proc Natl Acad Sci USA 107: 4477–4482

Walch-Liu P, Ivanov II, Filleur S, Gan Y, Remans T, Forde BG (2006) Nitrogen regulation of root branching. Ann Bot 97: 875–881

Wang D, Pei K, Fu Y, Sun Z, Li S, Liu H, Tang K, Han B, Tao Y (2007) Genome-wide analysis of the auxin response factors (ARF) gene family in rice (Oryza sativa). Gene 394: 13–24

Wang S, Li S, Liu Q, Wu K, Zhang J, Wang S, Wang Y, Chen X, Zhang Y, Gao C et al. (2015) The OsSPL16-GW7 regulatory module determines grain shape and simultaneously improves rice yield and grain quality. Nat Genet 47: 949–954

Wang S, Wu K, Qian Q, Liu Q, Li Q, Pan Y, Ye Y, Liu X, Wang J, Zhang J et al. (2017) Non-canonical regulation of SPL transcription factors by a human OTUB1-like deubiquitinase defines a new plant type rice associated with higher grain yield. Cell Res 27: 1142–1156

Wang S, Wu K, Yuan Q, Liu X, Liu Z, Lin X, Zeng R, Zhu H, Dong G, Qian Q et al. (2012) Control of grain size, shape and quality by OsSPL16 in rice. Nat Genet 44: 950–954

Wu K, Wang S, Song W, Zhang J, Wang Y, Liu Q, Yu J, Ye Y, Li S, Chen J et al. (2020) Enhanced sustainable green revolution yield via nitrogen-responsive chromatin modulation in rice. Science 367: eaaz2046

Wu MF, Tian Q, Reed JW (2006) Arabidopsis microRNA167 controls patterns of ARF6 and ARF8 expression, and regulates both female and male reproduction. Development 133: 4211–4218

Xi ZY, He FH, Zeng RZ, Zhang ZM, Ding XH, Li WT, Zhang GQ (2006) Development of a wide population of chromosome single-segment substitution lines in the genetic background of an elite cultivar of rice (Oryza sativa L.). Genome 49: 476–484

Xia X, Fan X, Wei J, Feng H, Qu H, Xie D, Miller AJ, Xu G (2015) Rice nitrate transporter OsNPF2.4 functions in low-affinity acquisition and long-distance transport. J Exp Bot 66: 317–331

Xiao HM, Cai WJ, Ye TT, Ding J, Feng YQ (2018) Spatio-temporal profiling of abscisic acid, indoleacetic acid and jasmonic acid in single rice seed during seed germination. Anal Chim Acta 1031: 119–127

Xu G, Fan X, Miller AJ (2012) Plant nitrogen assimilation and use efficiency. Annu Rev Plant Biol 63: 153–182

Yan M, Fan X, Feng H, Miller AJ, Shen Q, Xu G (2011) Rice OsNAR2.1 interacts with OsNRT2.1, OsNRT2.2 and OsNRT2.3a nitrate transporters to provide uptake over high and low concentration ranges. Plant Cell Environ 34: 1360–1372

Yang Y, Zhang J, Cai Z (2015) Nitrification activities and N mineralization in paddy soils are insensitive to oxygen concentration. Acta Agric Scand 66: 272–281

Yu J, Xiong H, Zhu X, Zhang H, Li H, Miao J, Wang W, Tang Z, Zhang Z, Yao G et al. (2017) OsLG3 contributing to rice grain length and yield was mined by Ho-LAMap. BMC Biol 15: 28

Zheng Z, Guo Y, Novak O, Dai X, Zhao Y, Ljung K, Noel JP, Chory J (2013) Coordination of auxin and ethylene biosynthesis by the aminotransferase VAS1. Nat Chem Biol 9: 244–246

Zhou F, Lin Q, Zhu L, Ren Y, Zhou K, Shabek N, Wu F, Mao H, Dong W, Gan L et al. (2013) D14-SCF(D3)-dependent degradation of D53 regulates strigolactone signalling. Nature 504: 406–410